HAQUE, M. & CAUGHLAN, C. N. (1966). *J. Amer. Chem. Soc.* **88**, 4124–4128.

HOKIN, L. E. & HOKIN, M. R. (1955). *Biochim. Biophys. Acta*, **18**, 102–110.

HOKIN, L. E. & HOKIN, M. R. (1958*a*). *J. Biol. Chem.* **233**, 818–821.

HOKIN, L. E. & HOKIN, M. R. (1958*b*). *J. Biol. Chem.* **233**, 805–814.

HOKIN, M. R. (1969). *J. Neurochem.* **16**, 127–134.

HOKIN, M. R., HOKIN, L. E. & SHELP, W. O. (1960). *J. Gen. Physiol.* **44**, 217–226.

IRVING, G. G. J. & COSGROVE, D. J. (1971). *Aust. J. Biol. Sci.* **24**, 559–564.

JEFFREY, G. A. & KIM, H. S. (1971). *Acta Cryst.* B**27**, 1812–1817.

JOHNSON, C. K. (1965). *ORTEP*. Oak Ridge National Laboratory Report ORNL-3794.

JOHNSON, L. F. & TATE, M. E. (1969). *Canad. J. Chem.* **47**, 63–73.

KARLE, I. L., HAUPTMAN, H., KARLE, J. & WING, A. B. (1958). *Acta Cryst.* **11**, 257–263.

KARLE, J. & HAUPTMAN, H. (1961). *Acta Cryst.* **14**, 217–223.

KOLLER, D., MAYER, A. M., POLJAKOFT-MAYBER, A. & KLEIN, S. (1962). *Ann. Rev. Plant Physiol.* **13**, 437.

LOMER, T. R., MILLER, A. & BEEVERS, C. A. (1963). *Acta Cryst.* **16**, 264–268.

LUNT, G. C., CANESSA, O. M. & DEROBERTS, E. (1971). *Nature, Lond.* **230**, 187–190.

PERUTZ, M. F. (1970). *Nature, Lond.* **228**, 726–739.

POSTERNAK, S. (1921). *Helv. Chim. Acta*, **4**, 150.

RABINOWITZ, I. N. & KRAUT, J. (1964). *Acta Cryst.* **17**, 159–168.

RIGGS, A. (1972). In *Biochemical Regulatory Mechanisms in Eukaryotic Cells*, pp. 1–31, edited by E. KUN & S. GRISOLIA. New York: Wiley–Interscience.

SHIONO, R. (1966*a*). *Data Reduction and Scaling FORTRAN Program*, Tech. Rpt., Crystallography Department, Univ. of Pittsburgh.

SHIONO, R. (1966*b*). *Modification of the Oak Ridge Least-Squares Program, ORFLS*, Tech. Rpt., Crystallography Department, Univ. of Pittsburgh.

SHIONO, R. (1969). *Wilson Plot Program for an IBM* 1130. Tech. Rpt., Crystallography Department, Univ. of Pittsburgh.

SHIONO, R. (1970). *Block-diagonal Least-squares Program*. Tech. Rpt., Crystallography Department, Univ. of Pittsburgh.

TEMPLETON, D. H. (1968). In *International Tables for X-ray Crystallography*, Vol. III, p. 213. Birmingham: Kynoch Press.

TRONIER, B., ORY, R. L. & HENNINGSEN, K. (1971). *Phytochemistry*, **10**, 1207–1211.

TRUTER, M. R. & TATE, M. E. (1970). *J. Chem. Soc.* (*B*), pp. 70–71.

VALIKHANOV, M. N. (1969). *Vopr. Fiziol. Biokhimikhlop.* pp. 3–9. *Chem. Abs.* **74**, 20443e.

WILLIAMS, S. G. (1970). *Plant Physiol.* **45**, 376–381.

Acta Cryst. (1975). B31, 2592

Structure and Binding in Molecular Complexes of Cyclic Polyethers. II.* Hydrogen Bonding and Ion Pairing in a Complex of a Macrocyclic Polydentate Ligand with Butylamine at 120 K

BY ISRAEL GOLDBERG

Department of Chemistry,† *University of California, Los Angeles, California* 90024, *U.S.A.*

(*Received* 3 *March* 1975; *accepted* 14 *April* 1975)

The crystal structure of a 1:1 complex of a macrocyclic polydentate ligand (3,6,9,12,15-pentaoxa-21-carboxybicyclo[15,3,1]heneicosa-1(21),17,19-triene; $C_{17}H_{24}O_7$) with t-butylamine has been determined from three-dimensional intensity data collected on a four-circle diffractometer at 120 K. The crystal is orthorhombic, space group *Pnma*. There are four molecular units in the unit cell of dimensions a = 17·811 (3), b = 13·920 (2) and c = 8·763 (2) Å. The structure was solved by direct methods and refined by the least-squares procedure to a final R value 0·038 for 1791 observations above threshold. The ionic constituents of the complex are located on mirror planes. The large host and the smaller guest species are held together by N–H···O hydrogen-bonding and ion-pairing interactions, which also have an effect on the flexible molecular conformation of the substituted polyether moiety. The observed packing arrangement appears to be stabilized by a three-dimensional network of C–H···O interactions. The host–guest complex is characterized by a high degree of symmetry.

Introduction

The present work is part of a study of host–guest compounds that involve synthetic multiheteromacrocyclic moieties acting as hosts in reactions of molecular complexation. Recently, problems of design and synthesis of differently shaped host compounds and their properties have been discussed, and a variety of forces potentially available for binding large host molecules to smaller guest species have been outlined (Cram *et al.*, 1975). In the previous publication of this

---

* Part I: *Acta Cryst.* B31, 754–762.

† Contribution No. 3449.

series (Goldberg, 1975*a*) the role of relatively weak dipole–dipole interactions in determining structural relationships in such complexes has been demonstrated. Additional chemical systems are being currently investigated in order to explore further the nature of intermolecular interactions by which complexes of polydentate ligands are stabilized in the solid state.

We describe here the crystal and molecular structures of a complex between t-butylammonium ion and the cyclic polyether host (the systematic name: 3,6,9,12,15-pentaoxa-21-carboxybicyclo[15,3,1]heneicosa-1(21),17,19-triene), shown below in the form of its carboxylate anion,

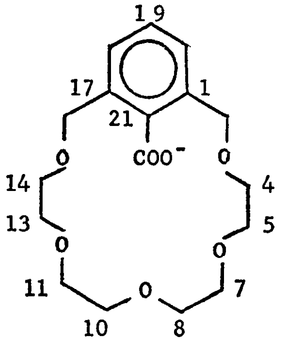

as determined from three-dimensional X-ray diffraction data collected at 120 K. The crystalline one-to-one salt was prepared by mixing the corresponding *acidic* form of the host with t-butylamine in a cyclohexane–dichloromethane solution (Newcomb & Cram, 1975). The crystal structure of the host molecule itself at ~120 K will be reported elsewhere. Several room-temperature crystal structures of alkali and alkaline earth complexes of polyether ligands have been reported (*e.g.*, Truter, 1973; Dunitz, Dobler, Seiler & Phizackerley, 1974).

Experimental

Single crystals of the title compound were kindly provided by Dr M. Newcomb. A preliminary survey of film data collected at room temperature indicated that the compound crystallized with orthorhombic symmetry. The systematic absences are $0kl$ with $k+l$ odd and $hk0$ with h odd, suggesting possible space group *Pnma* (D_{2h}^{16}) or $Pn2_1a$ (C_{2v}^{9}). A small crystal approximately 0·15 × 0·15 × 0·25 mm, glued to a glass fiber, was mounted on a Syntex $P\bar{1}$ diffractometer equipped with a gas-flow cooling device (Strouse, 1975), and was used to measure the cell constants and the intensities at the working temperature near 120 K. The temperature in the stationary N_2 stream at the position of the crystal was measured with a thin copper-constantan thermocouple.

Unit-cell dimensions determined from preliminary cone-axis and precession photographs were refined by a least-squares procedure applied to low-temperature measurements (15 reflections). The pertinent crystal data are given in Table 1.

Table 1. *Crystal data*

$(C_4H_{12}N)^+(C_{17}H_{23}O_7)^-$, M.W. 413·5, m.p. 117–126° (dec.)
Orthorhombic
$a = 17{\cdot}811\ (3)$, $b = 13{\cdot}920\ (2)$, $c = 8{\cdot}763\ (2)$ Å
$V = 2172{\cdot}6$ Å^3
$Z = 4$, $D_c(120\ \mathrm{K}) = 1{\cdot}264$ g cm^{-3}
$F(000) = 896$
Space group *Pnma* or $Pn2_1a$
$\mu(\mathrm{Cu}\ K\alpha) = 7{\cdot}8$ cm^{-1}

Intensity data were collected by the θ–2θ scan technique at a scan rate of 2° min^{-1} with graphite-monochromatized Cu $K\alpha$ ($\lambda = 1{\cdot}5418$ Å) radiation. The background to scan-time ratio was 0·8, and the 2θ range over the peak width was 1·0° below $K\alpha_1$ and above $K\alpha_2$. Three standard reflections (221, 040, 104) were monitored frequently to check the stability of the system. No significant changes in the intensities of these reflections were observed.

Structure amplitudes were derived in the usual manner for 2281 unique observations [1791 reflections have $F_o^2 \geq 3\sigma(F_o^2)$] recorded within $2\theta = 156°$, $(\sin\theta/\lambda)_{\max} = 0{\cdot}635$ Å^{-1}. The intensity data were corrected for Lorentz and polarization factors, but absorption corrections were ignored since the linear absorption coefficient was small. The estimated standard deviation of the intensities $\sigma(I) = [\sigma_s^2(I) + (pI)^2]^{1/2}$, where σ_s is the standard deviation due to counting statistics, included an adjustment factor of $p = 0{\cdot}04$ to account for instrumental errors.

Determination and refinement of the structure

Considering the unit-cell contents ($Z = 4$) and the molecular symmetry observed in the crystal structure of the uncomplexed host molecule (Goldberg, 1975*b*) we tended *a priori* to assume the lower space symmetry ($Pn2_1a$) for the crystals of the complex. A centric intensity distribution was indicated, however, through the $N(z)$ (Howells, Phillips & Rogers, 1950) and intensity moment (Foster & Hargreaves, 1963) tests, suggesting that the probable space group is *Pnma*, which requires a highly ordered arrangement of both ionic species in the unit cell. The subsequent structure analysis confirmed this. Approximate scale and overall isotropic temperature ($B = 2{\cdot}2$ Å^2) factors were evaluated by Wilson's method. The values of the statistical averages of calculated normalized structure factors (E_{hkl}) were 0·756 and 1·045 for $\langle|E|\rangle$ and $\langle|E^2-1|\rangle$, respectively. The structure was solved by multisolution weighted tangent-formula refinement (Germain, Main & Woolfson, 1971) of 266 reflections with $|E| \geq 1{\cdot}60$. Some difficulties were experienced in choosing a good starting set in the automated procedure, before it was decided to consider seven strong sign indications derived from the $\sum_1$ formula as known phases. These phases were zero for 040, 0,12,0, 006 and π for 0,10,0, 0,14,0, 004, 008 reflections. An E map based on a solution with the highest figure of merit ABSFOM (1·09) and the lowest RESID index (32·8) revealed clearly the positions of all non-hydrogen atoms in the chosen asymmetric unit. At this stage the agreement index R [$R=\sum(F_o-K|F_c|)/\sum F_o$ with K as a scale factor] for 382 low-angle reflections ($\sin\theta/\lambda\leq 0·35$) was 0·17.

Refinement was done by the least-squares method, minimizing $\sum w(\Delta F)^2$ [where $w=1/\sigma^2(F_o)$ and $\Delta F=F_o-K|F_c|$]. Two cycles in the block-diagonal approximation with individual isotropic temperature factors resulted in $R=0·115$ for 753 low-order reflections ($\sin\theta/\lambda\leq 0·45$). Anisotropic refinement of the heavy-atom structure based on a larger data set (1222 reflections with $F_o^2\geq 3\sigma(F_o^2)$, $\sin\theta/\lambda\leq 0·55$) reduced R to 0·098. At this point the 19 unique hydrogen atoms were clearly located on a difference Fourier synthesis, the corresponding peak-heights ranging from 0·55 to 0·90 e Å^{-3}. Three hydrogen atoms H(11), H(16*a*) and H(18*b*) (Table 3) were found to occupy special positions in the unit cell, as required by the assumed symmetry. Sections of the difference map computed in planes perpendicular to the N(16)–C(17), C(17)–C(18) and C(17)–C(19) bonds are shown in Fig. 1; they indicate that the $-NH_3^+$ and the methyl groups of the guest ion are ordered in the crystal structure.

Parameters adjusted in several subsequent cycles of full-matrix least-squares calculations included, therefore, coordinates and isotropic temperature factors of all the hydrogen atoms as well as the positional and anisotropic thermal parameters of the heavy atoms, and the scale factor. After these computations the refinement was considered completed since the average ratio of shift to e.s.d. for the adjusted parameters was less than 0·04 in the final cycle. The final discrepancy indices based on 1791 reflections above threshold are

Table 2. *Fractional coordinates and thermal parameters U^{ij} (Å^2) for the heavy atoms*

The e.s.d.'s are given in parentheses in units of the last decimal place. The anisotropic temperature is in the form $\exp[-2\pi^2(h_ia^i)\times(h_ja^j)U^{ij}\times 10^{-4}]$, where h_i and a^i are reflection indices and reciprocal unit-cell edges respectively.

	x	y	z	U^{11}	U^{22}	U^{33}	U^{12}	U^{23}	U^{13}
O(1)	0·0460 (1)	0·25	0·1818 (2)	192 (6)	260 (8)	311 (8)	0	0	−37 (6)
C(2)	0·0026 (1)	0·3342 (1)	0·1559 (2)	253 (7)	284 (8)	267 (8)	38 (6)	3 (6)	−46 (6)
C(3)	0·0523 (1)	0·4205 (1)	0·1714 (2)	421 (9)	299 (8)	237 (8)	−25 (7)	20 (6)	−79 (6)
O(4)	0·0712 (1)	0·4336 (1)	0·3282 (1)	311 (5)	256 (5)	238 (6)	−25 (4)	4 (4)	−29 (4)
C(5)	0·1100 (1)	0·5223 (1)	0·3539 (2)	291 (7)	207 (7)	293 (9)	33 (6)	−18 (6)	−8 (6)
C(6)	0·1928 (1)	0·5156 (1)	0·3228 (2)	300 (7)	187 (7)	242 (8)	27 (5)	35 (6)	−15 (5)
O(7)	0·2270 (1)	0·4607 (1)	0·4423 (1)	301 (5)	203 (5)	213 (6)	59 (4)	8 (4)	11 (4)
C(8)	0·3019 (1)	0·4309 (1)	0·4045 (2)	245 (7)	173 (6)	261 (8)	−17 (5)	−20 (5)	−17 (5)
C(9)	0·3021 (1)	0·3369 (1)	0·3193 (2)	164 (6)	167 (6)	193 (7)	−2 (4)	−3 (5)	−2 (4)
C(10)	0·2966 (1)	0·3360 (1)	0·1606 (2)	236 (7)	193 (6)	199 (7)	−1 (5)	27 (5)	20 (5)
C(11)	0·2937 (1)	0·25	0·0797 (2)	273 (10)	232 (10)	171 (10)	0	0	18 (7)
C(12)	0·3057 (1)	0·25	0·4000 (2)	137 (8)	192 (8)	163 (9)	0	0	2 (6)
C(13)	0·3150 (1)	0·25	0·5727 (2)	192 (8)	180 (8)	200 (10)	0	0	−11 (7)
O(14)	0·2556 (1)	0·25	0·6498 (2)	221 (7)	382 (8)	182 (8)	0	0	21 (5)
O(15)	0·3799 (1)	0·25	0·6239 (2)	204 (7)	643 (12)	240 (9)	0	0	−55 (6)
N(16)	0·1250 (1)	0·25	0·4988 (2)	180 (7)	263 (9)	197 (9)	0	0	26 (6)
C(17)	0·0690 (1)	0·25	0·6275 (2)	195 (9)	234 (9)	194 (10)	0	0	39 (7)
C(18)	−0·0097 (1)	0·25	0·5610 (2)	193 (9)	287 (11)	249 (11)	0	0	26 (8)
C(19)	0·0831 (1)	0·3403 (1)	0·7217 (2)	332 (8)	336 (8)	285 (9)	−24 (7)	−104 (6)	31 (7)

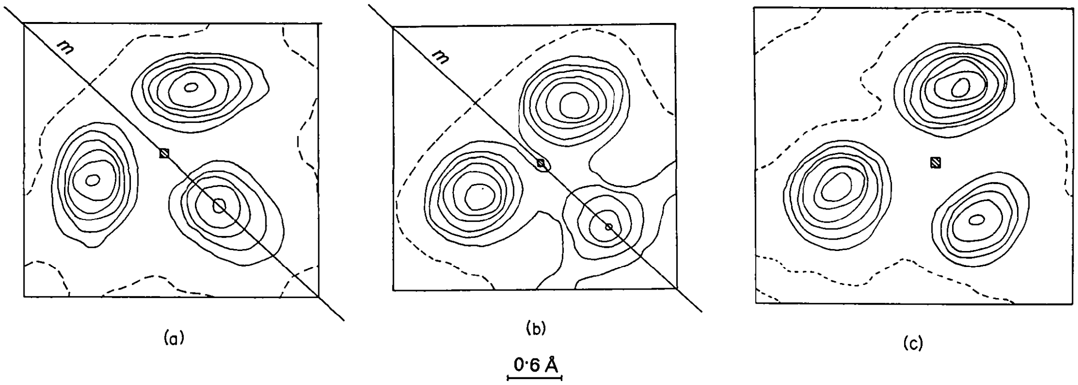

Fig. 1. General sections of a difference map computed in planes perpendicular to (*a*) C(17)–N(16), (*b*) C(17)–C(18) and (*c*) C(17)–C(19) in order to locate hydrogen atoms of the ammonium and methyl groups. Each square represents the projection of the C–N or C–C bond on the map. Contour intervals around each peak are 0·1 e Å^{-3} and start from 0·3 e Å^{-3}, except for the dotted line, which is the zero-density contour.

$R=0.038$ and $r=0.0024$ $[r=\sum w(\Delta F)^2/\sum wF_o^2]$.* The value of $[\sum w(\Delta F)^2/(n-m)]^{1/2}$ is 1·6 for $n=1791$ and $m=218$. When the very strong 014 reflection, the intensity of which was not accurately measured, and six weak reflections with $|F_c|<2$ are omitted, $R=0.037$ and $r=0.0022$.

The distribution of $\langle w(\Delta F)^2\rangle$ with increasing $\sin\theta/\lambda$ appeared reasonably constant. Most of the 11 highest peaks (0·13–0·22 e Å^{-3}) observed on a final difference map are close to the centers of the carbon–carbon bonds in both molecules. These features may reflect the errors introduced into the structural model by use of standard spherical atomic form factors (Kistenmacher, Rand & Marsh, 1974). The estimated standard deviation in the calculated Fourier syntheses is 0·02 e Å^{-3}.

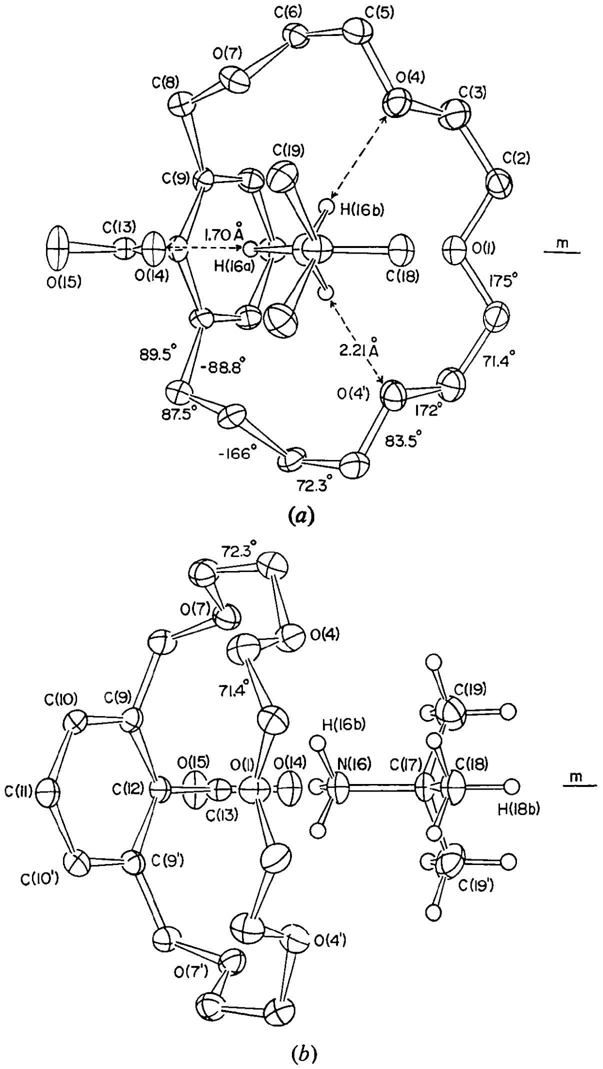

Fig. 2. Two views of the molecular unit. In (*a*) N(16)–C(17) is nearly perpendicular to the plane of the projection. Dihedral angles about the peripheral bonds are shown, the values −88·8° and 89·5° referring to torsion angles O(7′)–C(8′)–C(9′)–C(10′) and O(7′)–C(8′)–C(9′)–C(12) respectively. This figure, with 50% probability thermal ellipsoids, was produced with the aid of the program *ORTEP* (Johnson, 1965).

Table 3. *Atomic parameters for the hydrogen atoms*

The numbering of each hydrogen atom corresponds to that of the carbon or nitrogen atom to which the hydrogen is bonded.

	x	y	z	U (Å^2)
H(2*a*)	−0·040 (1)	0·337 (1)	0·229 (2)	0·031 (5)
H(2*b*)	−0·020 (1)	0·332 (1)	0·051 (2)	0·028 (5)
H(3*a*)	0·025 (1)	0·479 (1)	0·135 (2)	0·039 (5)
H(3*b*)	0·101 (1)	0·413 (1)	0·105 (2)	0·038 (6)
H(5*a*)	0·100 (1)	0·539 (1)	0·465 (2)	0·024 (5)
H(5*b*)	0·088 (1)	0·575 (1)	0·287 (2)	0·025 (5)
H(6*a*)	0·215 (1)	0·582 (1)	0·317 (2)	0·034 (5)
H(6*b*)	0·201 (1)	0·484 (1)	0·219 (2)	0·025 (5)
H(8*a*)	0·329 (1)	0·424 (1)	0·505 (2)	0·024 (5)
H(8*b*)	0·326 (1)	0·483 (1)	0·346 (2)	0·029 (5)
H(10)	0·295 (1)	0·398 (1)	0·102 (2)	0·033 (5)
H(11)	0·290 (1)	0·25	−0·033 (3)	0·036 (8)
H(16*a*)	0·176 (1)	0·25	0·543 (3)	0·033 (7)
H(16*b*)	0·120 (1)	0·304 (1)	0·436 (2)	0·040 (6)
H(18*a*)	−0·019 (1)	0·307 (1)	0·493 (2)	0·038 (5)
H(18*b*)	−0·048 (1)	0·25	0·647 (3)	0·031 (7)
H(19*a*)	0·048 (1)	0·342 (1)	0·810 (2)	0·033 (5)
H(19*b*)	0·136 (1)	0·340 (1)	0·761 (2)	0·042 (6)
H(19*c*)	0·075 (1)	0·402 (1)	0·660 (2)	0·035 (5)

The final heavy-atom parameters and their e.s.d.'s are given in Table 2, those of the hydrogen atoms in Table 3. The standard deviations of the parameters were estimated from the corresponding diagonal elements of the inverse matrix of the normal equations. Atomic scattering factors were taken from Hanson, Herman, Lea & Skillman (1964) for carbon, nitrogen and oxygen and from Stewart, Davidson & Simpson (1965) for hydrogen.

In this series of studies we have customarily assigned in least-squares refinement zero weights to very weak observations. The diffraction data contain relatively high background contributions and include a significant number of negative observed intensities; for the present structure these comprise about 8% of the total data set, and about one third of the intensities with $F_o^2\le 3\sigma(F_o^2)$. In view of Hirshfeld & Rabinovich's (1973) discussion of the treatment of weak observations in least-squares calculations, we decided to examine to what extent the parameters found for this structure are affected by elimination of weak reflections.

In two additional cycles of full-matrix calculations based on F^2, all the data (excluding the 014 reflection) were included, therefore, with positive weights. Some of the results resembled those reported by Hirshfeld & Rabinovich. The discrepancy index R rose to 0·054, and the standard deviations of the refined positional and thermal parameters were systematically increased

---

* The structure factor tables have been deposited with the British Library Lending Division as Supplementary Publication No. SUP 31071 (7 pp.). Copies may be obtained from The Executive Secretary, International Union of Crystallography, 13 White Friars, Chester CH1 1NZ, England.

by an average factor of 1·2. However, few parameters (mostly U's) changed by amounts exceeding twice the values of their estimated standard deviations. The resulting effect on molecular geometry and spatial intermolecular relationships in the crystal was not significant; all the bond lengths, bond angles, and nonbonded distances were within one e.s.d. of previous results. The description of atomic and molecular thermal vibrations was also very similar to that based on the 'truncated' data set. Examination of the difference density map recalculated at this stage indicated that the weak reflections contributed mainly to an increase in the background noise without showing any additional features that appear to be significant. It seems reasonable to conclude that imperfections in the experimental technique and in the model used influence the structurally interesting parameters much more than do distortions of the normal distribution of errors in the diffracted intensity pattern because of an arbitrary exclusion of very weak observations.

Results and discussion

Hydrogen bonding and crystal packing

The geometry of the complex is determined by a specific pattern of hydrogen bonding as shown on Fig. 2(*a*) and (*b*). The five oxygen atoms of the macro-ring and O(14) are arranged alternately below and above their least-squares plane (plane III, Table 7) in a manner somewhat similar to that observed in complexes involving a hexaether 18-membered macrocyclic moiety (Dunitz *et al.*, 1974; Goldberg, 1975*a*). This arrangement provides a symmetric electronegative cavity in the host for binding the guest ammonium ion. Atoms O(4), O(4′) and O(14) are primarily involved in hydrogen bonds with the $-NH_3^+$ group. In particular, the very short distances O(14)···N(16) (2·676 Å) and O(14)···H(16*a*) (1·70 Å) reflect a strong binding interaction, the main contribution coming from the opposite charges of the ammonium and the carboxylate groups. In fact, rarely have shorter intermolecular nonbonding nitrogen–oxygen or hydrogen–oxygen contacts been reported (*e.g.*, Fuller, 1959). The average $NH_n^+\cdots O$ hydrogen bond length observed in crystals is 2·83 Å (Wallwork, 1962; Donohue, 1968). Other relevant geometrical details (Table 4) include distances O(4)···N(16) 3·112 and O(4)···H(16*b*) of 2·21 Å, and angles N(16)–H(16*a*)···O(14) of 170° and N(16)–H(16*b*)···O(4) of 160°.

The N(16)–C(17) bond is almost perpendicular to the least-squares plane of the six oxygen atoms, the angle between the normal to this plane and the C–N bond being 3·4°. Presumably, direct polar nitrogen–oxygen interactions contribute also to the binding between the unlike species of the complex, although the O(7)···N(16) nonbonding contact (3·485 Å) is relatively large (see below). The non hydrogen-bonded O(1)···N(16) distance is 3·113 Å, identical to the hydrogen-bonded O(4)···N(16) distance.

A view of the crystal structure down the *b* axis (Fig. 3) shows several features of interest regarding the packing. In the unit cell, the polyether and the t-butylammonium, species are situated on mirror planes perpendicular to **b** at $y=\frac{1}{4}$ and $y=\frac{3}{4}$. Equivalent molecular units on the same plane, related by the *a* glide symmetry at $z=\frac{1}{4}$ or $z=\frac{3}{4}$ (*e.g.* molecules with shaded bonds in Fig. 3), are connected *via*

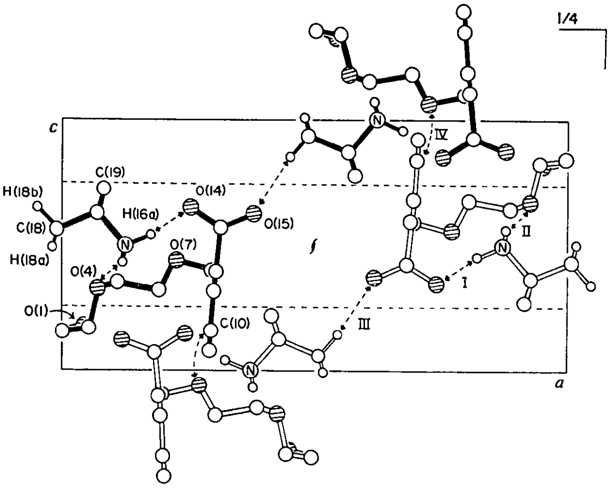

Fig. 3. Molecular packing. View of four equivalent molecules down the *b* axis, including symbols for some of the symmetry elements. For clarity, other units (related by a simple translation to those shown) are omitted from the unit-cell frame. The marked contacts represent intra-complex hydrogen bonds, (I) and (II), and inter-complex C–H···O 'bonds', (III) and (IV), described in Table 3.

Table 4. *Geometry of the* N–H···O *and the* C–H···O *interactions*

	R–H···O–R′ (at x,y,z)	(at i)	i	R–H (Å)	R···O (Å)	H···O (Å)	R–H···O (°)	R···O–R′ (°)
I.	N(16)–H(16*a*)···O(14)	–C(13)	x,y,z	0·98	2·676	1·70	170	117·8
II.	N(16)–H(16*b*)···O(4)	—C(3)	x,y,z	0·94	3·112	2·21	160	115·6
		—C(5)						119·0
III.	C(18)–H(18*b*)···O(15)	–C(13)	$x-\frac{1}{2},\frac{1}{2}-y,\frac{3}{2}-z$	1·02	3·390	2·38	170	146·7
IV.	C(10)–H(10)···O(7)	—C(8)	$\frac{1}{2}-x,1-y,z-\frac{1}{2}$	1·00	3·442	2·45	171	118·6
		—C(6)						86·0

In (II) the dihedral angle between planes *a* [defined by C(3), O(4), C(5)] and *b* [by N(16), H(16*b*), O(4)] is 89°; the N···O line forms an angle of 48° with the normal to *a*. In (IV) the dihedral angle between planes *c* [defined by C(6), O(7), C(8)] and *d* [by C(10), H(10), O(7)] is 81°; the C···O line forms an angle of 30° with the normal to *c*.

C–H···O interactions to form a zigzag chain crossing the glide plane and running parallel to the *a* axis in the crystal. The C(18)-methyl group of the guest and the carboxylate O(15)-oxygen atom are involved in these interactions (Table 4). In addition, relatively short C–H···O contacts, all lying close to and roughly parallel to the *n* glide planes of the structure, are observed between neighboring host molecules characterized by a difference of $\frac{1}{2}$ in the y coordinate of their centers. The corresponding O(7)···C(10*) [C(10*) is related to C(10) by a symmetry operation $\frac{1}{2}-x$, $1-y$, $\frac{1}{2}+z$] and O(7)···H(10*) distances are 3·442 and 2·45 Å respectively, and the C–H···O angle is 171°. Each host moiety participates in four interactions of this kind [*via* atoms O(7), O(7′), C(10) and C(10′)]. There are no other short contacts in the structure.

The existence of specific C–H···O interactions has been indicated in structural (*e.g.*, Mathew & Palenik, 1974; Bernstein, Cohen & Leiserowitz, 1974) as well as in theoretical (*e.g.*, Bonchev & Cremaschi, 1974) studies. It has been shown in the previous paper of this series that similar interactions between methyl groups and ether–oxygen atoms are strong enough to stabilize host–guest complexation in the solid state. In the present structure, the geometry of both types of C–H···O lateral contacts seems to be consistent with the expected spatial arrangement for a 'normal' hydrogen bond between hydrogen atoms and orbitals containing nonbonded electrons on oxygen (Table 4). The H···O distances (2·38 and 2·45 Å, values based on the experimental but underestimated C–H bond lengths) are slightly shorter than the sum of the corresponding van der Waals radii; they are, however, longer than the H···O distances in the intra-complex N–H···O hydrogen bonds. If we assume that the energy of a weak C–H···O interaction is of the order of 0·6–1·0 kcal mole^{-1} (Bonchev & Cremaschi, 1974) the cooperative effect of such interactions may add a significant contribution to other forces in determining the packing arrangement even in room temperature structures. Since the generally accepted operational definition states that hydrogen bonding exists if the energy of the specific interaction is at least 1 kcal mole^{-1} (*e.g.*, Arnett, Mitchell & Murty, 1974), the nomenclature of the above-discussed lateral C–H···O contacts is, however, a matter of taste.

Table 5. *Bond distances* (Å)

O(1)—C(2)	1·422 (2)	C(2)—H(2*b*)	1·01 (2)
C(2)—C(3)	1·498 (2)	C(3)—H(3*a*)	1·00 (2)
C(3)—O(4)	1·427 (2)	C(3)—H(3*b*)	1·04 (2)
O(4)—C(5)	1·433 (2)	C(5)—H(5*a*)	1·01 (2)
C(5)—C(6)	1·503 (2)	C(5)—H(5*b*)	1·01 (2)
C(6)—O(7)	1·432 (2)	C(6)—H(6*a*)	1·01 (2)
O(7)—C(8)	1·437 (2)	C(6)—H(6*b*)	1·02 (2)
C(8)—C(9)	1·507 (2)	C(8)—H(8*a*)	1·01 (2)
C(9)—C(10)	1·394 (2)	C(8)—H(8*b*)	0·98 (2)
C(9)—C(12)	1·403 (2)	C(10)–H(10)	1·00 (2)
C(10)–C(11)	1·393 (2)	C(11)–H(11)	0·99 (3)
C(12)–C(13)	1·522 (3)	N(16)–H(16*a*)	0·98 (3)
C(13)–O(14)	1·256 (3)	N(16)–H(16*b*)	0·94 (2)
C(13)–O(15)	1·240 (3)	C(18)–H(18*a*)	1·01 (2)
N(16)–C(17)	1·506 (3)	C(18)–H(18*b*)	1·02 (3)
C(17)–C(18)	1·518 (3)	C(19)–H(19*a*)	1·00 (2)
C(17)–C(19)	1·524 (2)	C(19)–H(19*b*)	1·00 (2)
C(2)—H(2*a*)	0·99 (2)	C(19)–H(19*c*)	1·03 (2)

Table 6. *Bond angles* (°)

C(2)—O(1)–C(2′)	111·0 (1)	C(9)—C(10)–C(11)	121·2 (1)
O(1)—C(2)–C(3)	109·0 (1)	C(10)–C(11)–C(10′)	118·6 (2)
C(2)—C(3)–O(4)	109·2 (1)	C(9)—C(12)–C(9′)	119·2 (2)
C(3)—O(4)–C(5)	112·0 (1)	C(9)—C(12)–C(13)	120·4 (1)
O(4)—C(5)–C(6)	113·0 (1)	C(12)–C(13)–O(14)	116·4 (2)
C(5)—C(6)–O(7)	108·5 (1)	C(12)–C(13)–O(15)	117·4 (2)
C(6)—O(7)–C(8)	112·4 (1)	O(14)–C(13)–O(15)	126·2 (2)
O(7)—C(8)–C(9)	111·5 (1)	N(16)–C(17)–C(18)	108·9 (2)
C(8)—C(9)–C(10)	120·2 (1)	N(16)–C(17)–C(19)	107·3 (1)
C(8)—C(9)–C(12)	119·9 (1)	C(18)–C(17)–C(19)	111·1 (1)
C(10)–C(9)–C(12)	119·9 (1)	C(19)–C(17)–C(19′)	111·1 (2)

Primed atoms are related to unprimed atoms (at x,y,z) by a mirror symmetry plane at $y=\frac{1}{4}$.

Molecular dimensions and conformation

Bond lengths and angles in both species, along with the estimated standard deviations, are listed in Tables 5 and 6. As reported in many other structures (*e.g.*, Goldberg, 1975*a*) the peripheral C–C bonds in the polyether macro-ring (1·498 and 1·503 Å) are shorter than the usually quoted reference value for a single C(sp^3)–C(sp^3) bond (1·537 Å; Sutton, 1965), while the adjacent carbon–oxygen bonds are of normal length, averaging 1·433 Å. Other dimensions are in the range of values documented in the literature for similar functional groups. Bond distances in the carboxylate group [C(13)–O(14), 1·256 Å; C(13)–O(15), 1·240 Å] indicate that the charge of the anion is delocalized on both carbon–oxygen bonds. The fact that C(13)–O(14) is, however, slightly but significantly longer correlates well with other indications that O(14) takes part in a stronger hydrogen-bonding interaction. Bond angles in the host moiety are also in the range of expected values.

The t-butylammonium ion forms a tetrahedron with N–C–C and C–C–C average angles of 108·1 and 111·1° respectively, and with distances of 1·506 Å for the N(16)–C(17) bond and of 1·518 and 1·524 Å for the carbon–carbon bonds. The nitrogen–carbon bond length in the present determination is characteristic of C(sp^3)–N distances observed in structures of ammonium salts and similar ionic species (in neutral molecules an average value of 1·47 Å is quoted for such bonds).

The observed values of the C–H bond lengths range from 0·98 to 1·04 Å with an average of 1·01 ± 0·01 Å. All H–C–H and H–N–H bond angles are in the range from 105 to 109°.

The conformation of the host is best illustrated in Figs. 2 and 3, and best described in terms of the torsion angles about the ring bonds (Fig. 2). The plane of the phenyl substituent (the benzene ring is planar within 0·01 Å) is perpendicular to that of the carboxylate group, eliminating any interaction between the π-electron systems of the two groups. The angle between the normal to the plane of the phenyl and the normal to the least-squares plane of the 18-membered ring is 66°. This angle is much smaller in the uncomplexed polyether molecule (Goldberg, 1975*b*); the larger value in the present structure provides a more favorable conformation for the host–guest complexation. The carboxylate and ammonium ions are on the same side of the macro-ring, allowing a strong ion-pairing interaction.

The ring conformation is significantly distorted from the symmetric 'crown' model observed in some previous studies because of the geometric constraints imposed by incorporation of the *m*-xylyl unit into the host moiety, and of the complexation with the guest ion. The ethyleneoxy units keep, however, their *gauche* conformation, the torsion angles about the corresponding carbon–carbon bonds being 71 and 72°.

The O···O distances within the six-oxygen cavity in the host show that O(7) deviates the most from the center of the hexagon (mainly along the *b* axis). The resulting distance of this oxygen from the centered ammonium group is significantly longer than the other N···O contacts. Examination of some relevant interatomic distances, and comparison with corresponding geometric details of the uncomplexed polyether molecule suggest that intramolecular steric repulsion may not be the main reason for the observed distortion. Since minor conformational changes in the macroring are usually of low energy, it seems likely that the involvement of O(7) in the intermolecular C–H···O interaction, as well as a twisting to optimize the N–H···O hydrogen bonding, affect the shape of the cavity.

The conformation of the t-butylammonium ion is characterized by an almost ideal staggered arrangement of the hydrogen-bonded ammonium hydrogen atoms relative to the three methyl carbons (Fig. 2*a*). Other hydrogens are positioned in such a way as to minimize all H···H repulsive interactions (Fig. 2*b*); all distances between hydrogen atoms bonded to different heavy atoms are greater than 2·5 Å. The resulting minimum-energy conformation and the pattern of N–H···O and C–H···O interactions both contribute to the ordered arrangement of the guest ion in the crystal structure.

Table 7 summarizes several least-squares planes of different parts of the structure.

Thermal motion

Rigid-body motion analysis of the vibration tensors of the nonhydrogen atoms was carried out by the method of Schomaker & Trueblood (1968) with the aid of a computer program written by Shmueli (1972). The agreement between the observed and calculated U^{ij} is poor, in accord with results reported by others for flexible polyether macrocyclic species (Dunitz *et al.*, 1974; Goldberg, 1975*a*). The discrepancy between the experimental and calculated parameters (corrected for the number of degrees of freedom) is $\langle(\Delta U^{ij})^2\rangle^{1/2}=$ 0·0045 Å^2 when all heavy atoms of the host moiety are included in the rigid body. The corresponding estimated value of $\langle\sigma^2(U^{ij})\rangle^{1/2}$ is 0·0007 Å^2. Different values of the r.m.s. ΔU^{ij} were obtained when the $-CO_2^-$ group was excluded from the analysis (0·0034 Å^2), and for the 18-membered ring fragment (0·0036 Å^2). The improvement of fit achieved by removing the carboxylate group indicates that its thermal motion is somewhat independent. Large-amplitude 'wagging' vibrations of both oxygen atoms [in particular of O(15)] parallel to the *b* axis (Fig. 2) correlate well with the fact that a large amount of free space is available in that direction.

Results of the analysis for the 21-atom fragment are summarized briefly in Table 8. They indicate that the overall pattern of thermal motion of this group is mainly of a translational character. The r.m.s. amplitudes of the assumed rigid-body libration are rather small, and consequently bond-length corrections for libration do not exceed 0·001 Å. On the other hand, the effects of possible torsional ring vibrations on the molecular geometry are unknown.

Conclusions

The present structure serves as a model for an important class of host–guest complexes of macro-

Table 7. *Least-squares planes*

x,y,z are fractional coordinates of a point in the plane and the right-hand side is the distance of the plane from unit-cell origin. The primed atoms are related to unprimed atoms by $x,\frac{1}{2}-y,z$.

Plane	Atoms defining the plane	Equation of the plane	Deviations from plane (Å)
I	C(9)–C(12), C(9′), C(10′)	$17{\cdot}762x-0{\cdot}647z=5{\cdot}164$	C(9)–C(12) < 0·01; O(7), −1·42; C(8), −0·06; C(13), 0·06; O(14), −1·05; O(15), 1·18
II	O(1)–C(9), C(2′)–C(9′), C(12)	$-6{\cdot}010x+8{\cdot}249z=1{\cdot}638$	O(1), −0·41; O(4), 0·64; O(7), 0·65; C(12), −0·18; O(14), 2·19; N(16), 1·73
III	O(1), O(4), O(7), O(14), O(4′), O(7′)	$-10{\cdot}981x+6{\cdot}900z=1{\cdot}085$	O(1), −0·34; O(4), 0·40; O(7), −0·53; O(14), 0·59; N(16), 0·98
IV	O(1), O(4), O(7), O(4′) O(7′)	$-8{\cdot}576x+7{\cdot}680z=1{\cdot}545$	O(1), −0·54; O(4), 0·37; O(7), −0·09; C(12), −1·09; N(16), 1·21
V	O(4), O(7), O(4′), O(7′)	$-6{\cdot}038x+8{\cdot}244z=2{\cdot}276$	O(1), −1·05; C(12), −0·82; N(16), 1·08
VI	O(1), O(4), O(4′)	$16{\cdot}812x-2{\cdot}894z=0{\cdot}247$	C(11), 4·46; C(12), 3·74
VII	C(18), C(19), C(19′)	$-11{\cdot}555x+6{\cdot}669z=3{\cdot}853$	O(4), −2·49; O(14), −2·47; N(16), −1·97

The angle between normals to planes (I) and (II) is 66°, (I) and (III) is 48°, (I) and (VI) is 15°, (III) and (VII) is 2°, (V) and (VI) is 51°.

Table 8. *Results of rigid-body motion analysis*

The results below are for the host moiety excluding the $-CO_2^-$ fragment. The eigenvectors of **L** and **T** and of the molecular system **I** are given in terms of the corresponding direction cosines which refer to the orthogonal axes *a*, *b* and *c*. Components of the origin shifts $\boldsymbol{\rho}(\rho_1,\rho_2,\rho_3)$ referred to the molecular centroid are given in Å.

	Eigenvalues	Eigenvectors		
	1326 (at.wt.Å^2)	0	1	0
[I]	1765	0·9804	0	0·1969
	2655	0·1969	0	−0·9804
	2·4 deg.^{2}	0	1	0
[L]	2·2	0·8016	0	0·5979
	1·6	0·5979	0	−0·8016
	231 × 10^{-4} Å^2	0·9931	0	−0·1174
[T]	194	0	1	0
	171	0·1174	0	0·9931

$\boldsymbol{\rho}(0{\cdot}98, 0, 1{\cdot}06)$

$\langle(\Delta U)^2\rangle^{1/2} = 0{\cdot}0034$ Å^2

cyclic polyethers in which a polar functional group is substituted on the host. In this compound the substituent is directed towards the polyether cavity, acting also (after proton-transfer) as an internal counter ion for the ionic guest. Host–guest structural relationships are affected by the resulting strong ion-pairing interactions.

The geometry of the complex is characterized by a very high organization. The molecular units occupy symmetry sites in the crystal, 12 atoms (including three hydrogens) lying on the mirror plane. This rather unexpected crystal packing of non-rigid species (rotational vibrations in t-butylammonium and torsional vibrations in the macro-ring are of relatively low energy) may be attributed to several factors. Among them are: a symmetric arrangement of the potential ligating sites with respect to the overall shape of the molecular unit, the geometry and shape of the guest ion, the steric compatibility between the hexagonal cavity formed and the dimensions of the cation, and the involvement of the planar carboxylate anion in multiple intermolecular interactions. The balance between the free energy needed to 'organize' the conformation of the host in order to meet the various geometrical requirements of feasible intermolecular interactions and the energy-gain derived therefrom is obviously favorable, leading to formation of this crystal structure. It is possible, therefore, that the present example demonstrates also an additional consequence of host–guest interaction in reactions of molecular complexation, where the larger product (complex) has a higher degree of symmetry than the constituent reactants in their stable form.

The molecular structure of the host reveals an interesting detail. The 18-membered ring contains only five oxygen atoms that are available for binding the guest ion by means of hydrogen bonds and nitrogen-oxygen, polar interactions. The host species adopted, however, a conformation in which a symmetric hexagonal cavity is formed (in fact, examination of space-filling models indicates that a different model of the structure, with the guest ion and the carboxylate group situated on opposite sides of the macro-ring, seems to be also acceptable.) It has been shown recently that higher-symmetry arrangements of ligating sites in the host cavity are usually associated with significantly higher binding constants of the host–guest products (Cram *et al.*, 1975). The observed coordination around the $-NH_3^+$ group in the present structure is consistent with those observations (see also Dunitz *et al.*, 1974; Newcomb & Cram, 1975).

The author is very grateful to Professor K. N. Trueblood for his constant encouragement and valuable criticism. He also wishes to thank Professor D. J. Cram and Dr M. Newcomb for helpful discussions and for providing the sample of the complex. All calculations were performed on the I.B.M. 360/91 Computer of the U.C.L.A. Campus Computing Network.

This investigation was supported by National Science Foundation Grant No. GP 32324X.

References

Arnett, E. M., Mitchell, E. J. & Murty, T. S. S. R. (1974). *J. Amer. Chem. Soc.* **96**, 3875–3891.

Bernstein, J., Cohen, M. D. & Leiserowitz, L. (1974). *The Chemistry of Quinonoid Compounds*, edited by S. Patai. New York: John Wiley.

Bonchev, D. & Cremaschi, P. (1974). *Theoret. Chim. Acta*, **35**, 69–80.

Cram, D. J., Helgeson, R. C., Sousa, L. R., Timko, J. M., Newcomb, M. E., Moreau, P., De Yong, F., Gokel, G. W., Hoffman, D. H., Domeier, L. A., Peacock, S. C., Madan, K. & Kaplan, L. (1975). *Pure Appl. Chem.* In the press.

Donohue, J. (1968). *Structural Chemistry and Molecular Biology*, pp. 443–465, edited by A. Rich & N. Davidson. San Francisco: Freeman.

Dunitz, J. D., Dobler, M., Seiler, P. & Phizackerley, R. P. (1974). *Acta Cryst.* B**30**, 2733–2738.

Foster, F. & Hargreaves, A. (1963). *Acta Cryst.* **16**, 1133–1139.

Fuller, W. (1959). *J. Phys. Chem.* **63**, 1705–1717.

Germain, G., Main, P. & Woolfson, M. M. (1971). *Acta Cryst.* A**27**, 368–376.

Goldberg, I. (1975*a*). *Acta Cryst.* B**31**, 754–762.

Goldberg, I. (1975*b*). *Acta Cryst.* To be published.

Hanson, H. P., Herman, F., Lea, J. D. & Skillman, S. (1964). *Acta Cryst.* **17**, 1040–1044.

Hirshfeld, F. L. & Rabinovich, D. (1973). *Acta Cryst.* A**29**, 510–513.

Howells, E. R., Phillips, D. C. & Rogers, D. (1950). *Acta Cryst.* **3**, 210–214.

Johnson, C. K. (1965). *ORTEP*. Oak Ridge National Laboratory Report ORNL- 3794.

Kistenmacher, T. J., Rand, G. A. & Marsh, R. E. (1974). *Acta Cryst.* B**30**, 2573–2578.

Mathew, M. & Palenik, G. J. (1974). *Acta Cryst.* **B30**, 2381–2385.
Newcomb, M. & Cram, D. J. (1975). *J. Amer. Chem. Soc.* **97**, 1257–1259.
Schomaker, V. & Trueblood, K. N. (1968). *Acta Cryst.* **B24**, 63–76.
Shmueli, U. (1972). *TMA. Thermal Motion Analysis*, Department of Chemistry, Tel-Aviv Univ., Tel-Aviv.
Stewart, R. F., Davidson, E. R. & Simpson, W. T. (1965). *J. Chem. Phys.* **42**, 3175–3187.
Strouse, C. E. (1975). To be published.
Sutton, L. E. (1965). *Tables of Interatomic Distances and Configuration in Molecules and Ions.* Supplement. Spec. Publ. No. 18. London: The Chemical Society.
Truter, M. R. (1973). *Struct. Bond.* **16**, 71–111.
Wallwork, S. C. (1962). *Acta Cryst.* **15**, 758–759.

Acta Cryst. (1975). B31, 2600

Die Kristallstruktur von Bis-(*N*,*N*′-diäthylthioselenocarbamato)-kupfer(II)

Von J. Kaiser, R. Richter und J. Sieler
*Sektion Chemie der Karl-Marx-Universität, DDR-*701 *Leipzig, Liebigstrasse* 18, *DDR*

(*Eingegangen am* 19. *November* 1974; *angenommen am* 4. *April* 1975)

The crystal and molecular structure of bis-(*N*,*N*′-diethylthioselenocarbamato)copper(II) has been determined by single-crystal X-ray diffraction methods. The structure was solved by conventional Patterson and Fourier heavy-atom techniques followed by block-diagonal least-squares refinement which resulted in an R value of 0·13 for 2040 independent reflexions from Weissenberg photographs. The crystals are monoclinic with space group $P2_1/c$ and cell dimensions (Guinier data) $a=9{\cdot}575$ (6), $b=11{\cdot}245$ (6), $c=16{\cdot}791$ (8) Å, $\beta=112{\cdot}89$ (8)° and $Z=4$. The copper atom is located inside a tetragonal pyramid of chalcogen atoms which consists of two centrosymmetrically related molecules of the complex. Its position is 0·27 Å above the base of two sulphur and two selenium atoms in a *trans* position and 2·884 Å below a fifth atom (selenium) belonging to the second molecule of the pair. The other average bond distances are Se–C 1·82, S–C 1·83, C–N 1·36 and N–C 1·49 Å.

In den letzten Jahren wurden von Newman & White (1972), Peyronel, Pignedoli & Antolini (1972), Agre & Shugam (1972) und anderen Röntgenkristallstrukturanalysen von Dithiocarbamatkomplexen (Ligand dtc$^-$) mit Übergangsmetallen publiziert. Demgegenüber gibt es nur wenige Arbeiten (Bonamico & Dessy, 1971; Noordik & Smits, 1974) über Strukturbestimmungen von Diselenocarbamaten (Ligand dsc$^-$).

Tanaka & Sonoda (1971) sowie Heber, Kirmse & Hoyer (1972) synthetisierten Komplexe mit dem Liganden Thioselenocarbamat (tsc$^-$). Wir untersuchten das Bischelat Cu(tsc)$_2$, wobei im Laufe der Strukturbestimmung ein Teil der ursprünglich publizierten Kristalldaten (Kaiser, Hoyer & Höhne, 1972) korrigiert werden musste. Die Kristallstruktur von Cu(tsc)$_2$, deren Parameter nach dem letzten Ver-

Tabelle 1. *Atomkoordinaten und anisotrope Temperaturfaktoren* (× 10^4) *für* Cu(tsc)$_2$ *mit Standardabweichungen* (*e.s.d.*) *in Klammern*

Die Temperaturkoeffizienten b_{ij} sind durch den Ausdruck $T=\exp\left[-(b_{11}h^2+b_{22}k^2+b_{33}l^2+b_{12}hk+b_{13}hl+b_{23}kl)\right]$ gegeben.

	x	y	z	b_{11}	b_{22}	b_{33}	b_{23}	b_{13}	b_{12}
Cu(1)	1933 (3)	319 (3)	652 (2)	141 (4)	78 (6)	43 (1)	−12 (3)	65 (3)	−15 (6)
Se(2)	3441 (3)	2187 (3)	1081 (2)	178 (4)	120 (5)	57 (1)	−9 (3)	85 (3)	−16 (6)
S(3)	2019 (4)	625 (5)	2057 (2)	76 (4)	13 (8)	20 (1)	−9 (4)	22 (4)	−13 (7)
S(4)	2583 (5)	−313 (6)	−487 (3)	128 (5)	20 (9)	30 (2)	−13 (5)	74 (5)	−36 (9)
Se(5)	730 (3)	−1698 (3)	315 (2)	164 (3)	108 (5)	45 (1)	−1 (3)	69 (4)	−5 (5)
N(6)	372 (2)	270 (2)	276 (1)	116 (23)	111 (32)	45 (7)	−17 (22)	54 (21)	−29 (38)
N(7)	139 (1)	−265 (2)	−101 (1)	92 (16)	38 (26)	27 (5)	−13 (16)	36 (14)	2 (27)
C(8)	313 (2)	194 (2)	207 (1)	99 (19)	36 (33)	30 (6)	26 (20)	47 (18)	−17 (34)
C(9)	465 (2)	375 (3)	277 (2)	211 (35)	40 (48)	67 (12)	−34 (33)	112 (33)	−99 (57)
C(10)	357 (2)	244 (3)	359 (1)	121 (39)	123 (39)	31 (9)	−45 (26)	32 (24)	−76 (45)
C(11)	358 (3)	480 (3)	243 (2)	208 (41)	124 (50)	68 (13)	−74 (37)	92 (38)	−16 (64)
C(12)	486 (3)	160 (3)	418 (2)	147 (42)	151 (51)	72 (14)	−22 (38)	53 (39)	−52 (67)
C(13)	156 (2)	−170 (2)	−50 (1)	119 (22)	36 (35)	36 (7)	3 (22)	60 (20)	−17 (38)
C(14)	214 (2)	−267 (3)	−164 (1)	179 (29)	77 (42)	38 (10)	−2 (29)	93 (27)	−29 (50)
C(15)	43 (3)	−375 (3)	−100 (1)	149 (30)	76 (44)	55 (10)	−9 (29)	74 (28)	−3 (50)
C(16)	107 (3)	−242 (3)	−257 (2)	194 (37)	115 (48)	47 (12)	−42 (35)	63 (34)	−133 (61)
C(17)	139 (3)	−480 (3)	−52 (2)	197 (37)	134 (46)	62 (12)	−14 (35)	116 (35)	54 (60)